Dendrochronologia 86 (2024) 126229

Contents lists available at ScienceDirect

Dendrochronologia

journal homepage: www.elsevier.com/locate/dendro

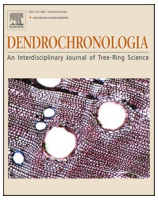

An integration of μXRF and X-ray microdensitometry records in dendrochronology

Samuli Helama [a,*], Timo Saarinen [b], Tapio Suominen [b], Mauricio Fuentes [c], Thomas Frank [d], Björn E. Gunnarson [e,f]

[a] Natural Resources Institute Finland, Rovaniemi, Finland
[b] Geology, Department of Geography and Geology, University of Turku, Turku, Finland
[c] Regional Climate Group, Department of Earth Sciences, University of Gothenburg, Gothenburg, Sweden
[d] Department of Earth Sciences, Uppsala University, Uppsala, Sweden
[e] Department of Physical Geography, Stockholm University, Stockholm, Sweden
[f] Bolin Centre for Climate Research, Stockholm University, Stockholm, Sweden

ARTICLE INFO

Keywords:
Dendrochronology
Dendrochemistry
Microdensitometry
X-ray fluorescence
Latewood maximum density
Calcium concentration

ABSTRACT

X-ray based microdensitometry is conventionally used to produce climate-related tree-ring records. Micro X-ray fluorescence (μXRF) applications represent another growing area of interest and opportunities in dendrochronology. This paper demonstrates a method to correctly juxtapose and precisely synchronise the densitometry and μXRF profiles. Among μXRF variables, full fluorescence spectrum (FFS) corresponds distinctly well with the microdensitometry-based wood density variations. Accordingly, the FFS provides the most applicable variable to integrate the μXRF and density profiles. The method proposed here can be used to demonstrate the strength and sign of μXRF variables and wood density relations. Moreover, the μXRF based records can be readily compared to density variables, such as the latewood maximum density, which is demonstrated in this paper.

1. Introduction

X-rays have been traditionally applied in dendrochronology for densitometry. Latewood maximum density (MXD) records, in particular, have been extensively produced for high-altitude and high-latitude sites where MXD data correlate strongly with summer temperature and provide more reliable temperature reconstructions and estimations of post-eruption climate anomalies than tree-ring widths (Briffa et al., 2002a, 2002b; Wilson et al., 2016; Anchukaitis et al., 2017). Moreover, at sites where tree growth is limited by water stress, MXD can be used as a proxy record for fluctuations in precipitation and moisture conditions (Rocha et al., 2020a). μXRF, in turn, can be used to accurately quantify abundances of chemical elements in research materials. In dendrochronology, the μXRF analyses are carried out by mapping the distribution of the elements over an area of tree-ring cross-section or by using line scanning along pith-to-bark radius to assess variations of elements as timeseries. Recent examples from dendrochronological studies show that μXRF can be applied to various research targets including, among others, monitoring of soil fertilizer treatments (Ortega Rodriguez et al., 2018), detection of climate signal in elemental records (Sánchez-Salguero et al., 2019), tracing anthropogenic contamination (Rocha et al., 2020b), and dating of elemental response to a volcanic event (Pearson et al., 2020).

Tree-ring density and chemistry both reflect changes in tree growth, wood anatomy, and ultimately climate. Combining chemical and wood density series can bring several benefits for tree-ring studies. Dendrochemical patterns of Ca and K were previously shown to identify physiological and anatomical processes that involve changes in element composition of wood, heartwood/sapwood and earlywood/latewood differentiation. Moreover, Fe, Zn, Cl, S and Ca were shown to portray anomalies linked to volcanic eruptions, in addition to ring-width and MXD (Hevia et al., 2018). In addition, relationships between ring-width, MXD and chemical data have been shown to vary between sites and trees growing on basic and acid soils (Sánchez-Salguero et al., 2019). More studies are required to demonstrate these linkages for different tree species. Previously, intra- and inter-annual patterns in Ca and Mn content and wood density were used to indicate annual tree-ring boundaries, however, the correlations between tree-ring width, density and concentrations of Ca, K and Mn were also found to be species-specific (Ortega Rodriguez et al., 2022). These studies confirm the potential of

* Correspondence to: Natural Resources Institute Finland, Ounasjoentie 6, Rovaniemi 96200, Finland.
E-mail address: samuli.helama@luke.fi (S. Helama).

https://doi.org/10.1016/j.dendro.2024.126229
Received 10 October 2023; Received in revised form 14 May 2024; Accepted 10 June 2024
Available online 6 July 2024

wood-chemistry studies based on μXRF, in combination with ring-width and density analyses, to identify the repertoire of physiological and anatomical processes driving changes in element composition within trees.

To demonstrate these linkages over secured timelines, it is beneficial to juxtapose and precisely synchronize the inter- and intra-annual patterns the density and elemental data exhibit, prior to any further inquiry. Moreover, similar to any dendrochronological data, the elemental profiles need to be cross-dated to assign each XRF point measurement to a specific annual ring and calendar year. The μXRF spectrometers have not, however, been primarily developed for tree-ring applications, and the setup in use may lack suitable means for cross-dating. When the count rates of fluorescent photons of elements and radiographic grey-scale images are simultaneously produced, the element specific count rates can be assigned to annual tree-ring patterns by an approach where the pixel-wise data output are related to ring boundaries (Hevia et al., 2018). Here, we consider the case where the two types of data have not been simultaneously produced. That is, given the density values have been cross-dated using standard dendrochronological techniques, direct synchronisation of the density and elemental profiles will result in correctly cross-dated elemental patterns. Such a synchronisation of the profiles, however, may not be a straightforward task when the profiles have not been obtained simultaneously. In such a case, the areas of analysed cross-sections may not be strictly identical as the specimen has been relocated from sample holder of an X-ray densitometry to that of an X-ray fluorescence spectrometer. Second, the intra-annual patterns that are commonly discerned in wood density and anatomy profiles (Schweingruber, 1990; Vaganov, 1990) may appear less obvious in elemental profiles, which impairs their comparisons to each other. It follows that it is necessary to find the μXRF variables that best correspond to observed changes in wood density. Third, we hypothesise that analysing the synchronised profiles may help to find μXRF variables that could support the dendrochronological studies traditionally relying on physical growth-based proxies. A goal of this approach would be to develop tree-ring based multi-proxy studies, relying on physical and chemical data.

Previous μXRF investigations have shown that concentrations of Ca, in particular, could illustrate intra-annual patterns that correspond with anatomical changes from earlywood to latewood (Silkin and Ekimova, 2012). Instead of single elements, however, a wide range of XRF spectra may offer an alternative tool for comparing the density and μXRF profiles. Here we hypothesise that such summation of elements and their concentrations could feasibly correspond to wood density, that similarly represents the concentration of all elements present in wood. Accordingly, full fluorescence spectrum (0–40 keV) represents a variable that can be derived from μXRF analyses and compared with density profiles. This variable represents the total number of emitted and scattered photons in the sample over the energy range 0–40 keV and could feasibly correspond to wood density, in which case the information on the element concentrations can be synchronised with density fluctuations and, subsequently, analysed along exactly the same transect of the same wood specimen. This comparison is carried out for a set of tree-ring samples obtained from living Scots pine (*Pinus sylvestris* L.) trees in northern Finnish Lapland and cross-dated using standard protocols, as previously published as a part of our recent palaeoclimate study (Helama et al., 2022). Here, these samples were exposed to μXRF analyses and compared with microdensitometry-based data.

2. Methods

2.1. Microdensitometry

MXD data were produced for a set of tree-ring samples (10 mm diameter core) from three living *P. sylvestris* trees using the standard protocols (Gunnarson et al., 2011) by an ITRAX Wood Scanner from Cox Analytic System (http://www.coxsys.se). The ITRAX Wood Scanner produces high-resolution radiographic images. Thin laths (1.20 mm thick) were cut from samples using a twin-bladed circular saw. The samples were treated with alcohol in a Soxhlet apparatus. This analytical step extracted resins and other removable compounds unrelated to wood density (Schweingruber et al., 1978). The laths were acclimatised to 12 % moisture content (air dry), mounted in the Wood Scanner, and exposed to a narrow, high energy, X-ray beam in 20 μm steps. The samples were X-rayed in the ITRAX machine equipped with a chrome tube tuned to 30 kV and 50 mA, with 75 ms step time. For each step, a sensor with a slit opening of 20 μm registered the radiation that was not absorbed by the sample. The Wood Scanner produced an 8-bit, gray-scale, digital image with a resolution of 2540 dpi. The grey levels were calibrated using a calibration wedge from Walesch Electronic. The radiographic images were evaluated using WinDENDRO tree-ring image processing software, which provides ring width and density data from a scanned image (Guay et al., 1992).

Samples may contain hollow and rotten parts. Density profiles were obtained from pith towards the bark through the lines avoiding these parts.

To cross-check the data, the ring widths from WinDENDRO were compared for each tree with ring-width data that had been measured under the light microscope and cross-dated against the existing master chronology (Helama et al., 2022). The resulting profile of maximum and minimum density and the mean densities of the earlywood, latewood and of each whole ring were recorded. The WinDENDRO software also allows to export the series of all density values within each pith-to-bark profile. In addition to the density values, such data contain information of calendar year the ring is dated to and whether the data-point belongs to earlywood or latewood. These data provided the density profiles that were compared with μXRF data in this study.

2.2. μXRF analysis

Materials used for the μXRF analysis were half-core samples retained from the densitometry analyses, i.e., the 'twin-samples' of each tree-ring core thus representing exactly the same radius of tree stem. In order to study the spatial variation of elements in tree-ring cross-sections, distribution maps of elements (2D maps) were produced by a Bruker M4 Tornado μXRF spectrometer with two silicon drift detectors and Rh anode. The spot size of capillary optics X-ray beam was c. 20 μm. After calibration of spectrometers with a Zr standard, the tree-ring samples were fixed on measurement stage and pressure of the chamber was dropped down to 20 mbar. High voltage of 50 kV and 600 μA current were used. The radial distance of the pixels was 20 μm. The exposure time was 10 ms/pixel. Hypermaps with spectra of all obtained pixels were exported for later analysis. Distribution maps of elements were based on investigation of the total spectrum. Most distinct energy peaks of Kα and Lα were used to identify elements from the samples. In practice, the information depth varies with both the sample matrix and atomic number of the fluorescing element, being lower for those with low atomic number (e.g. Bartoll et al., 2003; Flude et al., 2017). 2D maps were investigated with different filters to produce maps illustrating the concentration of elements. To assess the average elemental composition of radial variation of elements, line scan analysis was conducted. An analysis line was drawn from the innermost part near the pith towards the outer rings (i.e., line scan route intersecting the ring boundaries). The values of the pixels perpendicular to the line within 0.4 mm were summed to remove the noise, which may be occurring if very narrow line width is used. As a limitation, the line may not optimally intersect all the ring boundaries. Albeit this was not a problem in the case of our samples, we note that the use of multiple lines may appear more suitable solution for samples with less regular ring patterns. The use of multiple lines may, on the other hand, be more prone to discords between the μXRF and density profiles due to less stable measurement tracks. Previous studies have used the μXRF machinery and methods identical to this study for various types of materials including, among others, annual

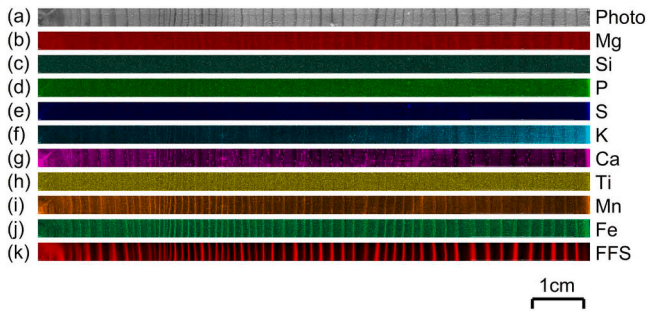

Fig. 1. A photo of our HAT015 tree-ring sample (a) and μXRF maps illustrating the concentration of elements (b–j) and full fluorescence spectrum (FFS) (k) in that sample.

increments of freshwater bivalve shells (Leppänen et al., 2021) and whitefish otoliths (Finnäs et al., 2022). Full fluorescence spectrum (FFS) was acquired over an energy range of 0–40 keV to obtain total X-ray intensity map of the analysed cross-section. This variable (FFS) represents the total number of the entire X-ray spectra and as such represents the total number of emitted and scattered photons in the sample over the energy range 0–40 keV. Moreover, the spectra of elements showing intra-annual variations, in visual inspection, that could be linked to structure of tree rings, were recorded.

2.3. Statistics behind the approach

Density and μXRF profiles from the same tree were compared statistically and visually. Visual inspection of the μXRF profiles (single elements and FFS) was performed to identify elements whose intra-annual variations mimicked tree-ring based growth patterns of the same sample. That is, the μXRF profiles with patterns corresponding to the growth fluctuations were selected for statistical analyses. Next, a cross-correlation analysis was carried out. The μXRF profile of each selected element was slid along the density profile to detect a position with no offset between the two data. The position with no offset was defined as follows. The density and μXRF values were scaled to mean of zero and standard deviation of one (z-scores) and the residual sum of squares was calculated between the two records. Statistically, the position with no offset was determined by the minimum of a sum of squares. In this study, density and μXRF profiles were both produced using radial step of 20 μm, which means that the two types of records were directly compared, with no need to adjust the distance between data points prior to the cross-correlation analysis. We note, however, that if resolution of

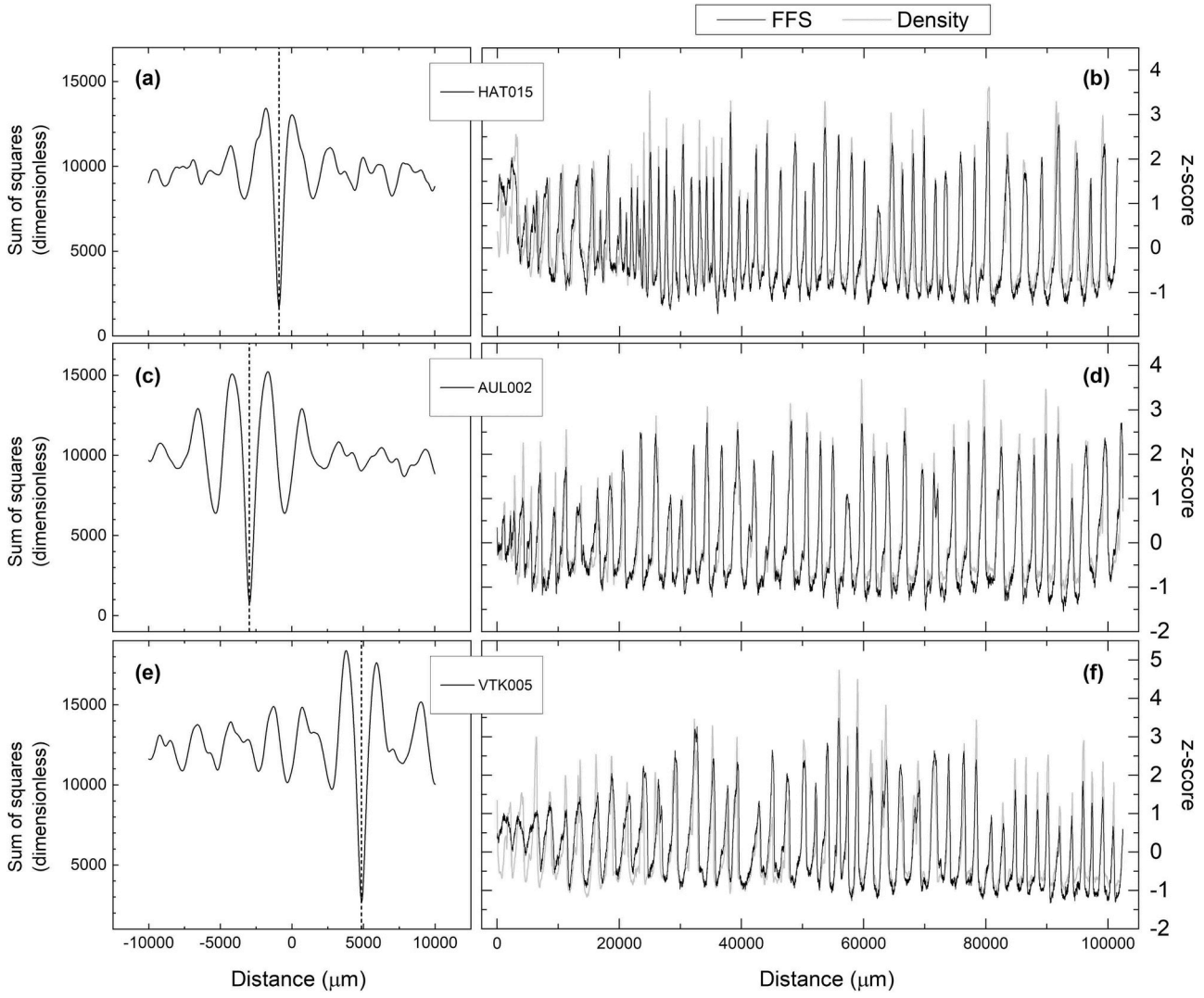

Fig. 2. Synchronisation of μXRF and microdensitometric records, represented by full fluorescence spectrum (FFS) and X-ray based wood density, respectively. Total sum of squares was calculated for a range of temporal positions (a, c, e) to detect a position with no offset between the two data (b, d, f). Vertical dotted line denotes the position of the minimum of a sum of squares. The comparison is presented for our HAT015, AUL002 and VTK005 samples.

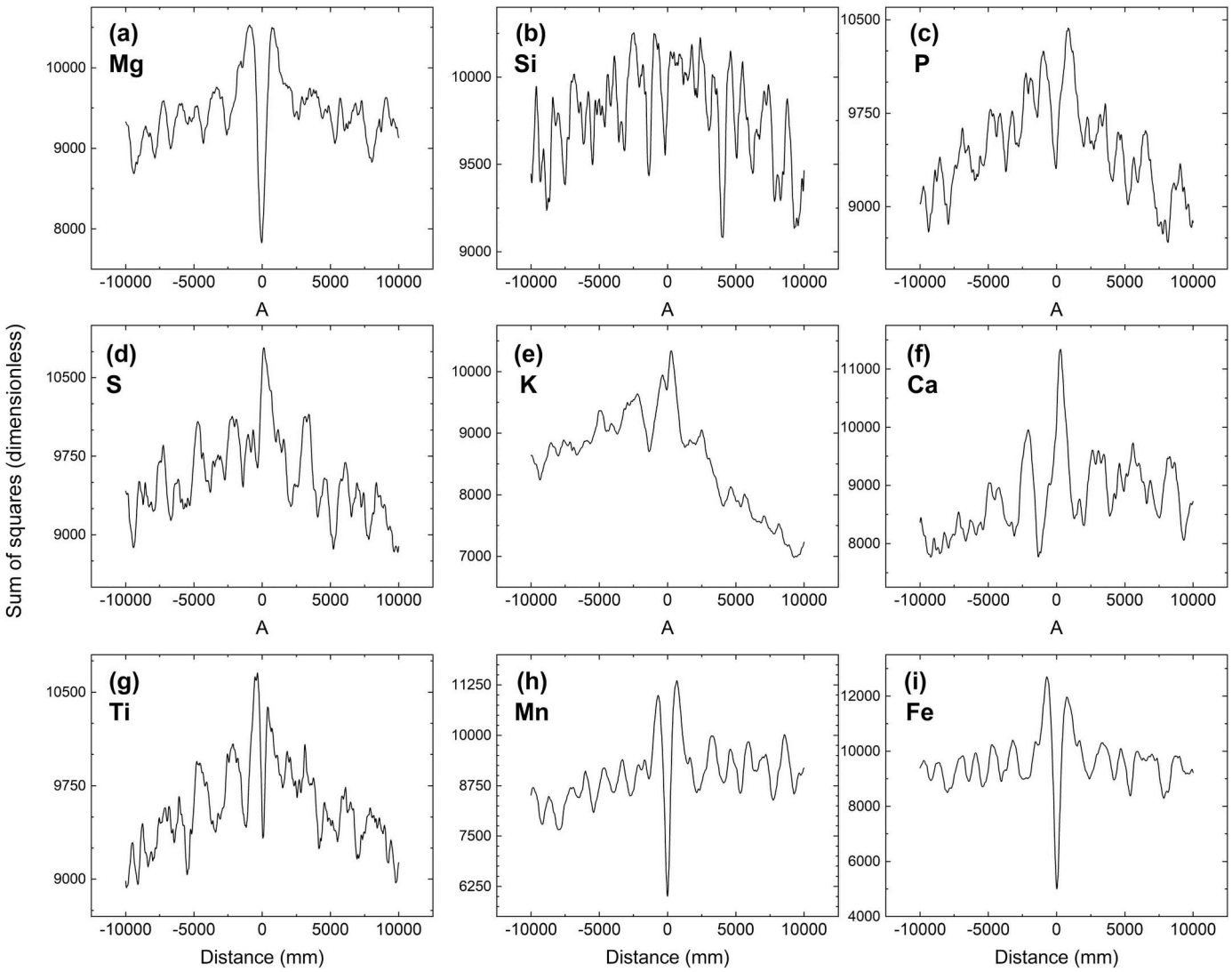

Fig. 3. Comparison of μXRF and microdensitometric records. Total sum of squares was calculated for a range of temporal positions for nine different elements subsequent to the synchronisation (see Fig. 2). The comparison is presented for our HAT015 sample. See Fig. S1 and S2 for identical comparisons of the samples AUL002 and VTK005.

the density and μXRF were not identical, as may be the case elsewhere, the x coordinate should be translated into comparable units before the profiles are being compared.

Once the μXRF and density records were synchronised, the μXRF data became simultaneously cross-dated against the inter- and intra-annual variations of density profile that had been correctly aligned to calendar years. A new set of μXRF data comparable to MXD records were produced. This was done by obtaining yearly maxima of FFS that is typically located in the latewood portion of each ring. That is, the quantification of annual FFS maxima mimicked closely that of annual density maxima i.e., MXD (Schweingruber et al., 1978; Schweingruber, 1990). In addition, similar sets of μXRF records were constructed by obtaining the yearly maxima of each analysed element. However, for those elements correlating negatively with density, the records were obtained as the yearly minima in that elemental data. The μXRF and MXD records were compared to each other using Pearson correlations (Sokal and Rohlf, 1981). For illustrative purposes, the annual data of μXRF variables were rescaled to mean and standard deviation of the MXD data. In the case of those elements correlating negatively with density, the data were multiplied by minus one prior to rescaling, to invert the records for improved visualisation.

3. Demonstration of the method

Visual inspection of the μXRF maps illustrated that concentration of several elements showed inter-and intra-annual variations that can be tentatively linked to structure of tree rings. The results of the elemental variations that show any traces of annual patterns are first viewed for our HAT015 sample (Fig. 1a–j). It is obvious that even among these most promising μXRF variables the annual pattern is more discernible for some elements that for others. In any case, visual inspection of the FFS map illustrated intra-annual variations that were more distinct than those observed for single elements (Fig. 1k).

For that same sample (HAT015), statistical comparison between the FFS and density records indicated a minimum of a sum of squares at a relative distance of 880 μm (Fig. 2a). Adjusting the position of the FFS record accordingly, the μXRF and density records became precisely synchronised (Fig. 2b). Similar approach could possibly be applied to at least some of the single elements, however, their comparisons did not result in such a distinct peak in the minimum of a sum of squares except for Mg, Mn and Fe (Fig. 3). Instead, some of the elements (S, K and Ca; see Fig. 3d–f) appeared to show maxima of a sum of squares (instead of minima) when the μXRF and density records were correctly aligned, indicating a negative correlation between the density and elemental

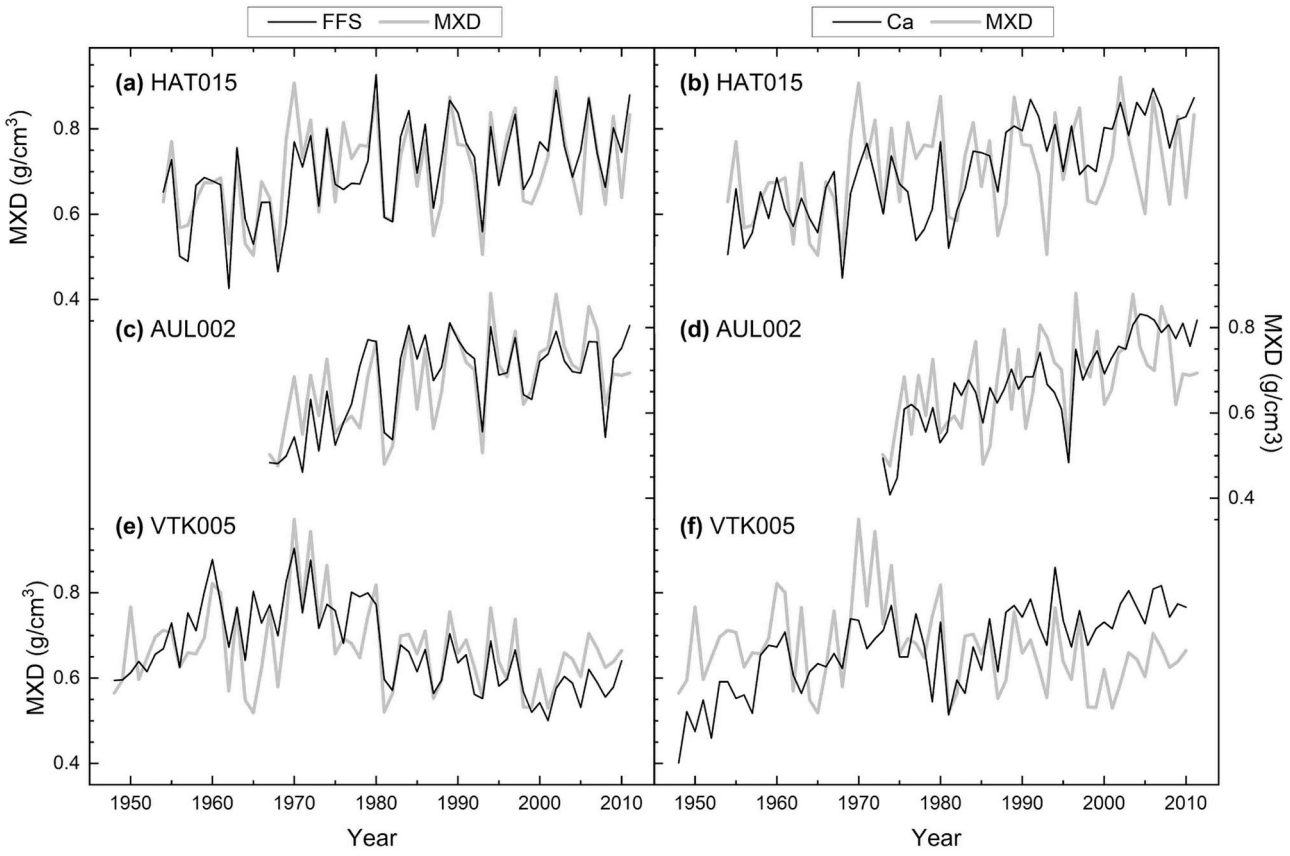

Fig. 4. Comparison of μXRF and microdensitometry-based latewood maximum density (MXD) records for HAT015 (a–b), AUL002 (c–d) and VTK005 (e–f) samples. The full fluorescence spectrum (FFS) (a, c, e) and Ca (b, d, f) data were rescaled to mean and standard deviation of the MXD data prior to comparison. Note that the scale of Ca data has been inverted to permit better visualisation.

variables.

Similar results were obtained for the remaining set of our samples. Accordingly, the data of the FFS profiles were used when the μXRF and density records were synchronised relative to the minimum of a sum of squares (Fig. 2c–f). Similar to our HAT015 sample, single elements did not indicate as strong and consistent relationship to wood density in comparison to FFS (Fig. S1 and S2).

The annual records of MXD and maximum FFS data correlated well with each other (Fig. 4). On average, the correlations between the maximum FFS and MXD data were $r = 0.79$. Here, records comparable to MXD were also accomplished using minimum Ca data (Fig. 4). Correlations of these data with MXD were in any case weaker (and negative). On average, the Ca versus MXD correlations were $r = -0.46$.

4. Summary and conclusions

In this technical note, we have demonstrated an intra- and inter-annual integration of μXRF and X-ray microdensitometry records. To this end, we introduced a method that can be used to illustrate the strength and sign of relations between the μXRF variables to wood density. The method may be particularly beneficial for situations where the μXRF and density profiles have been produced separately from same or paired samples and need to be correctly and precisely aligned, to connect the two types of profiles radially. Given that the microdensitometry-based wood density fluctuations have been cross-dated, which is an initial routine of any dendrochronological investigation, the application of the method results in simultaneously cross-dated μXRF-based chemistry data, demonstrating the radial concentrations of elements in the analysed tree-ring structures. Apart from single elements, the μXRF-based variable we analysed involved the full fluorescence spectrum (FFS). In our approach, this variable could be seen to act as a summation of elements and their concentrations. That is, FFS correlated more clearly and consistently with radial variations in wood density than any of the single elements, which is logical as the microdensitometry-based wood density is neither distinguishing between the concentrations of the elements. Once the μXRF and microdensitometry-based profiles have been precisely aligned, as done here by using the FFS, the inter- and intra-annually resolved records of single elements are ready to be compared with those of wood density. As a caveat, our investigation was limited to *Pinus sylvestris* samples, and more testing is warranted to explore different tree species and their ring types. With this in mind software application could be developed for the synchrony detection.

Our dendrochronological approach to μXRF and wood density data can be summarised as follows:

1. Wood chemistry and density information are produced using micro X-ray fluorescence spectrometer and microdensitometry, respectively.
2. Records of ring widths from WinDENDRO (or any other relevant software) are cross-dated against ring widths measured and cross-dated conventionally under the light microscope against the existing master chronology.
3. Pith-to-bark profiles of density values produced for tree-ring samples are exported from WinDENDRO.
4. Line scans through the 2D maps of elemental concentrations are produced for the same tree-ring samples, to derive μXRF-based data both on FFS (acquired here over an energy range of 0–40 keV) and elemental concentrations.

5. Density and FFS values are scaled to mean of zero and standard deviation of one (z-scores). The FFS profile is slid along the density profile of the same tree-ring sample to detect a position with no offset between the two data for statistical and visual comparison. Statistically, the position with no offset was determined by the minimum of a sum of squares.
6. The cross-dated μXRF-based records that are now correctly aligned to calendar years can be used in multi-proxy tree-ring studies based both on physical and chemical data.

Here, especially Ca data corresponded with density fluctuations, which concurred with findings of previous literature showing that concentrations of Ca illustrate intra-annual wood anatomical changes. These methodological findings set the stage for future comparisons of Ca and other elements, that could be linked to structure of tree rings and their density fluctuations, and ultimately to climatic and environmental variables with larger sets of samples, tree species and site conditions.

CRediT authorship contribution statement

Samuli Helama: Writing – review & editing, Writing – original draft, Visualization, Validation, Supervision, Project administration, Methodology, Investigation, Funding acquisition, Formal analysis, Conceptualization. **Mauricio Fuentes:** Writing – review & editing, Validation, Software, Methodology, Investigation, Formal analysis, Data curation, Conceptualization. **Thomas Frank:** Writing – review & editing, Software, Investigation, Formal analysis, Data curation. **Timo Saarinen:** Writing – review & editing, Visualization, Validation, Supervision, Software, Resources, Project administration, Methodology, Investigation, Funding acquisition, Formal analysis, Data curation, Conceptualization. **Tapio Suominen:** Writing – review & editing, Validation, Software, Methodology, Investigation, Formal analysis, Data curation, Conceptualization. **Björn E. Gunnarson:** Writing – review & editing, Validation, Supervision, Software, Resources, Project administration, Methodology, Investigation, Formal analysis, Data curation, Conceptualization.

Declaration of Competing Interest

The authors declare that they have no known competing financial interests or personal relationships that could have appeared to influence the work reported in this paper.

Data availability

Data will be made available on request.

Acknowledgements

This study was funded by the Academy of Finland.

Appendix A. Supporting information

Supplementary data associated with this article can be found in the online version at doi:10.1016/j.dendro.2024.126229.

References

Anchukaitis, K.J., Wilson, R., Briffa, K.R., Büntgen, U., Cook, E.R., D'Arrigo, R., Davi, N., Esper, J., Frank, D., Gunnarson, B.E., Hegerl, G., Helama, S., Klesse, S., Krusic, P.J., Linderholm, H.W., Myglan, V., Osborn, T.J., Zhang, P., Rydval, M., Schneider, L., Schurer, A., Wiles, G., Zorita, E., 2017. Last millennium Northern Hemisphere summer temperatures from tree rings: part ii, spatially resolved reconstructions. Quat. Sci. Rev. *163*, 1–22. https://doi.org/10.1016/j.quascirev.2017.02.020.

Bartoll, J., Unger, A., Püschner, K., Stege, H., 2003. Micro-XRF investigations of chlorine-containing wood preservatives in art objects. Stud. Conserv. *48*, 195–202. https://doi.org/10.1179/sic.2003.48.3.195.

Briffa, K.R., Osborn, T.J., Schweingruber, F.H., Jones, P.D., Shiyatov, S.G., Vaganov, E. A., 2002a. Tree-ring width and density data around the Northern Hemisphere: Part 1, local and regional climate signals. Holocene *12*, 737–751. https://doi.org/10.1191/0959683602hl587rp.

Briffa, K.R., Osborn, T.J., Schweingruber, F.H., Jones, P.D., Shiyatov, S.G., Vaganov, E. A., 2002b. Tree-ring width and density data around the Northern Hemisphere: Part 2, spatio-temporal variability and associated climate patterns. Holocene *12*, 759–789. https://doi.org/10.1191/0959683602hl588rp.

Finnäs, V., Lill, J.-O., Saarinen, T., Lindqvist, C., Heimbrand, Y., Jokikokko, E., Hägerstrand, H., 2022. Micro-X-ray fluorescence image analysis of otoliths to distinguish between wild-born and stocked river-spawning whitefish captured in the Baltic Sea. Fish. Manag. Ecol. *29*, 233–240. https://doi.org/10.1111/fme.12525.

Flude, S., Haschke, M., Storey, M., 2017. Application of benchtop micro-XRF to geological materials. Mineral. Mag. *81*, 923–948. https://doi.org/10.1180/minmag.2016.080.150.

Guay, R., Gagnon, R., Morin, H., 1992. A new automatic and interactive. Tree measurement system based on a line scan camera. For. Chron. *68*, 138–141. https://doi.org/10.5558/tfc68138-1.

Gunnarson, B.E., Linderholm, H.W., Moberg, A., 2011. Improving a tree-ring reconstruction from west-central Scandinavia: 900 years of warm-season temperatures. Clim. Dyn. *36*, 97–108. https://doi.org/10.1007/s00382-010-0783-5.

Helama, S., Herva, H., Arppe, L., Gunnarson, B., Frank, T., Holopainen, J., Nöjd, P., Mäkinen, H., Mielikäinen, K., Sutinen, R., Timonen, M., Uusitalo, J., Oinonen, M., 2022. Disentangling the evidence of milankovitch forcing from tree-ring and sedimentary records. Front. Earth Sci. *10* https://doi.org/10.3389/feart.2022.871641.

Hevia, A., Sánchez-Salguero, R., Camarero, J.J., Buras, A., Sangüesa-Barreda, G., Galván, J.D., Gutiérrez, E., 2018. Towards a better understanding of long-term wood-chemistry variations in old-growth forests: a case study on ancient *Pinus uncinata* trees from the Pyrenees. Sci. Total Environ. *625*, 220–232. https://doi.org/10.1016/j.scitotenv.2017.12.229.

Leppänen, J.J., Saarinen, T., Jilbert, T., Oulasvirta, P., 2021. The analysis of freshwater pearl mussel shells using μ-XRF (micro-x-ray fluorescence) and the applicability for environmental reconstruction. SN Appl. Sci. *3* https://doi.org/10.1007/s42452-020-03978-3.

Ortega Rodriguez, D.R., de Carvalho, H.W.P., Tomazello-Filho, M., 2018. Nutrient concentrations of 17- year-old *Pinus taeda* annual tree-rings analyzed by X-ray fluorescence microanalysis. Dendrochronologia *52*, 67–79. https://doi.org/10.1016/j.dendro.2018.09.009.

Ortega Rodriguez, D.R., Hevia, A., Sánchez-Salguero, R., Santini, L., de Carvalho, H.W.P., Roig, F.A., Tomazello-Filho, M., 2022. Exploring wood anatomy, density and chemistry profiles to understand the tree-ring formation in Amazonian tree species. Dendrochronologia *71*. https://doi.org/10.1016/j.dendro.2021.125915.

Pearson, C., Salzer, M., Wacker, L., Brewer, P., Sookdeo, A., Kuniholm, P., 2020. Securing timelines in the ancient Mediterranean using multiproxy annual tree-ring data. Proc. Natl. Acad. Sci. USA *117*, 8410–8415. https://doi.org/10.1073/pnas.1917445117.

Rocha, E., Gunnarson, B.E., Holzkämper, S., 2020a. Reconstructing summer precipitation with MXD data from *Pinus sylvestris* growing in the Stockholm archipelago. Atmosphere *11*. https://doi.org/10.3390/atmos11080790.

Rocha, E., Gunnarson, B., Kylander, M.E., Augustsson, A., Rindby, A., Holzkämper, S., 2020b. Testing the applicability of dendrochemistry using X-ray fluorescence to trace environmental contamination at a glassworks site. Sci. Total Environ. *720* https://doi.org/10.1016/j.scitotenv.2020.137429.

Sánchez-Salguero, R., Camarero, J.J., Hevia, A., Sangüesa-Barreda, G., Galván, J.D., Gutiérrez, E., 2019. Testing annual tree-ring chemistry by X-ray fluorescence for dendroclimatic studies in high-elevation forests from the Spanish Pyrenees. Quat. Int. *514*, 130–140. https://doi.org/10.1016/j.quaint.2018.09.007.

Schweingruber, F.H., 1990. Radiodensitometry. In: Cook, E.R., Kairiukstis, L.A. (Eds.), Methods of Dendrochronology: Applications in the Environmental Sciences. Kluwer Academic Publishers, Dordrecht, pp. 55–63.

Schweingruber, F.H., Fritts, H.C., Bräker, O.U., Drew, L.G., Schär, E., 1978. The X-ray technique as applied to dendroclimatology. Tree-ring Bull. *38*, 61–91.

Silkin, P.P., Ekimova, N.V., 2012. Relationship of strontium and calcium concentrations with the parameters of cell structure in Siberian spruce and fir tree-rings. Dendrochronologia *30*, 189–194. https://doi.org/10.1016/j.dendro.2011.06.003.

Sokal, R.R., Rohlf, F.J., 1981. Biometry, Second ed. W.H. Freeman, San Francisco, p. 859 (p).

Vaganov, E.A., 1990. The tracheidogram method in tree-ring analysis and its application. In: Cook, E.R., Kairiukstis, L.A. (Eds.), Methods of Dendrochronology: Applications in the Environmental Sciences. Kluwer Academic Publishers, Dordrecht, pp. 63–73.

Wilson, R., Anchukaitis, K., Briffa, K.R., Büntgen, U., Cook, E., D'Arrigo, R., Davi, N., Esper, J., Frank, D., Gunnarson, B., Hegerl, G., Helama, S., Klesse, S., Krusic, P.J., Linderholm, H.W., Myglan, V., Osborn, T.J., Rydval, M., Schneider, L., Schurer, A., Wiles, G., Zhang, P., Zorita, E., 2016. Last millennium northern hemisphere summer temperatures from tree rings: Part I: the long term context. Quat. Sci. Rev. *134*, 1–18. https://doi.org/10.1016/j.quascirev.2015.12.005.